

Article

# Impact Evaluation of Track Girder Bearing on Yeongjong Grand Bridge

**Jung-Youl Choi** <sup>1</sup> and **Sun-Hee Kim** <sup>2,\*</sup>

<sup>1</sup> Department of Railroad Construction & Safety Engineering, Dongyang University, No. 145 Dongyangdae-ro, Pugggi-eup, Yeongju-si 36040, Korea; [jychoi@dyu.ac.kr](mailto:jychoi@dyu.ac.kr)

<sup>2</sup> Department of Architectural Engineering, Gachon University, 1342 Seongnamdaero, Sujeong-gu, Seongnam-si 13120, Korea

\* Correspondence: [shkim6145@gachon.ac.kr](mailto:shkim6145@gachon.ac.kr); Tel.: +82-031-750-4718

Received: 13 November 2019; Accepted: 18 December 2019; Published: 20 December 2019



**Abstract:** The line track bearings used in the Yeongjong Grand Bridge experienced cracks and deformations, which result in significant accelerations and displacements of the track. This study measured an acceleration and a displacement of 0.5 g and 0.5 mm, respectively. Three-dimensional finite element analysis was performed to predict the behavior of railway tracks. However, when low-maintenance cylindrical bearings were used instead of line bearings, the displacement was decreased by 93%, and the acceleration was decreased by 82%. Furthermore, it turned out that the maximum displacement of the track girder was decreased by 45% when cylindrical bearings were used.

**Keywords:** line bearing; cylindrical bearing; dynamic behavior; railway bridge; the Yeongjong Grand Bridge

## 1. Introduction

Bridge bearings applied to a railway bridge are installed on a bridge deck, and they need to have a means of generating resistance to negative reaction forces to support a track and rails installed on top of the bridge. The track should not be allowed to be rotated perpendicular to the bridge using bridge bearings in order to prevent falling of trains; however, even when small amounts of such rotations are permitted, it should be supported with considerable forces. In the case of a one-way movable end, stretching due to thermal strain, etc. should be allowed in the bridge axis direction.

Bridge bearings include elastic bearings, steel bearings, pot bearings, disk bearings, spherical bearings, and seismic isolation bearings [1]. Line bearings are a type of steel bearing fabricated by casting for installation. They have a simple form, where one side of a junction is flat and the other is spherical for reduced frictional resistance and rotational displacement absorption [2]. Line bearings have a small bearing area for bearing support, which is likely to cause local damage to the bridge structure during load transfer. Further, these bearings have a short maintenance cycle owing to the wear of the joint, as all members that make up line bearings are made of steel [3]. These line bearings are used in a fixed end, in a movable end of less than 40 mm, or where the reaction force is not large. As they slide and move as per Hertzian contact theory, they suffer severe damage to the joint, and the friction coefficient may exceed significantly. Thus, it may be impossible to absorb and dissipate vibration generated during train operation, which may result in secondary damage such as train derailment caused by the transverse displacement of a track and rail surfaces resulting from the damage to a bearing block [4]. To solve such problems, research studies on bridge bearings are being actively conducted.

Choi et al. compared disk bearings with polyurethane (PTFE) disks by estimating the static and dynamic rigidity of the disk bearings through field tests and finite element analysis to solve the problems that occur in existing steel bearings. The static rigidity was found to be close to half of the estimated static rigidity under dynamic loading, and the dynamic behavior of the steel bearings turned out to be ~80% greater than the dynamic rigidity of the disk bearings with PTFE. Further, the gap inside the expansion bearing seemed to play a critical role in increasing deformation [3]. Choi and Choi measured the dynamic behavior of line bearings, spherical bearings, and disc bearings of a railroad plate girder as a train traveled and analyzed the dynamic behavior of a plate girder bridge with each bearing. As a result, the results showed the highest dynamic behavior with line bearings, and there was a difference in the amount of lifting at fixed and movable ends with disc bearings. With spherical bearings, similar lifting amounts were measured at fixed and movable ends, confirming that spherical bearings had elastic resistance against lifting [5]. Yau et al. applied train loads to a bridge with elastic bearings and conducted a numerical analysis of the shock. As a result, the dynamic response of the bridge remained constant, when damping effects were considered. When the elastic bearings were installed at the bridge point to isolate the seismic force, it was confirmed that the dynamic response of the bridge was adversely amplified against the moving train load [6]. Herwing and Brühwiler presented a simple model of fatigue and field measurements of the dynamic behavior of a railway bridge during the train service to analyze the complex elastic dynamic system. The cause of the dynamic effect on the fatigue of the bridge occurred in the vertical track position. The results of the study allow for the consideration of realistic dynamic amplification factors for fatigue verification [7]. Pan et al. evaluated the sensitivity of seismic response of a bridge with three-dimensional (3D) finite element analysis and parametric analysis for seismic vulnerabilities of multispan simply supported steel girders in New York. The simulation results indicated that it was more advantageous to retrofit the bridge by connecting the bridge and elastomeric bearings continuously [8]. Choi et al. performed experiments on the light dynamic behavior of the improved spherical bearings in a plate girder bridge and on the resistance to negative reaction forces. The behavioral differences were analyzed by measuring the dynamic behavior of the plate girder bridge in a state with line bearings and in a state after replacing them with spherical bearings. As a result, it was confirmed that the improved spherical bearings reduced the vertical deflection in the center of the plate girder bridge compared to the existing bearings, contributing to the improvement of the driving stability of the vehicle [9].

In the previous studies, long-span bridges have been actively conducted by Caprani et al. and Chen et al. [10,11]. However, the focus of this study is on the support of bearings for long-span simple-beam bridges of a track–bridge system.

In this study, field measurements and numerical analysis were performed to analyze the characteristics of the structural behavior of the track installed on the Yeongjong Grand Bridge based on the type of bearings and that of the bearings themselves.

## 2. Direct-Fixation Track Bearing System for the Yeongjong Grand Bridge

The Yeongjong Grand Bridge is a composite bridge that extends over a total of 4.42 km, and it comprises a 0.55 km suspension bridge, a 2.25 km truss bridge, and a 1.62 km steel-box girder bridge as shown in Figure 1. The suspension bridge built in the main route is the first 3D self-anchored suspension bridge in South Korea for roads and railways [12].

The direct-fixation rail-fastening system (Figure 2) employed on the Yeongjong Grand Bridge is a rail-fastening system that uses a leaf-spring-type fastener, an adjustable pad as the adjustment packing, and a loosening preventive nut instead of a general nut [12,13].

Figure 3 shows schematic views of the direct-fixation track on the Yeongjong Grand Bridge. On the left and right sides of the Yeongjong Grand Bridge, line bearings are installed as shown in Figure 3a. The direct-fixation track is in a structure, where 12.5 m long simple-beam-type track girders are placed continuously to support the rail, as shown in Figure 3b.

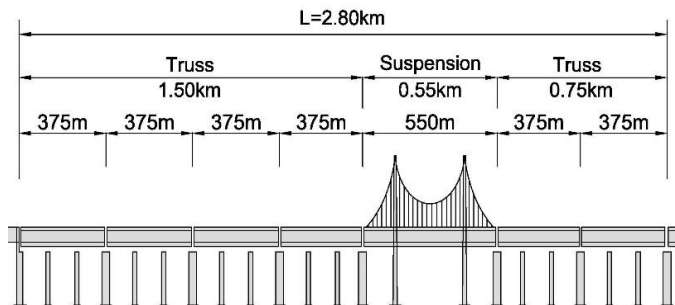


**Figure 1.** Scheme of a direct-fixation track on the Yeongjong Grand Bridge [12].

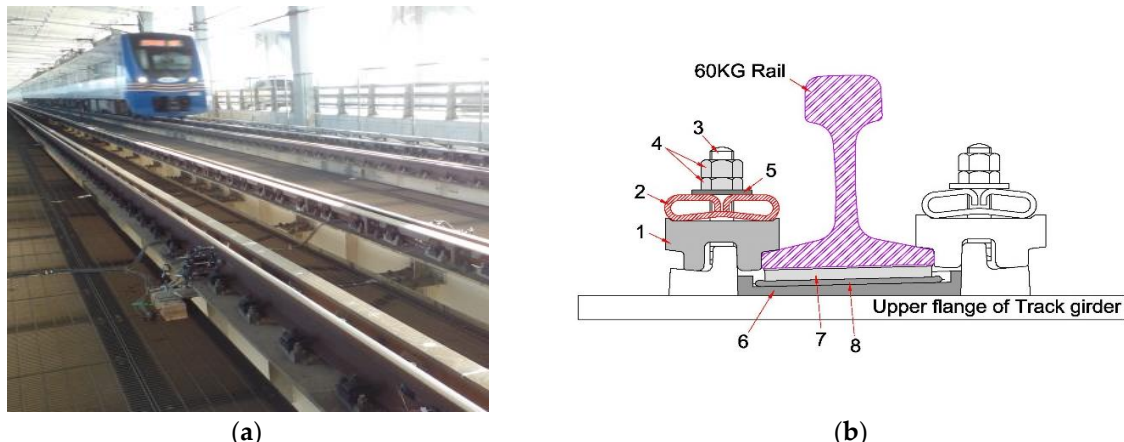


**Figure 2.** (a) Image of a direct-fixation rail-fastening system [12,13]. (b) The composition of the direct-fixation rail-fastening system: 1. insulation block; 2. leaf-spring-type fastener; 3. bolt; 4. loosening preventive nut; 5. washer; 6. insulation plate; 7. rail pad; and 8. adjustable pad.

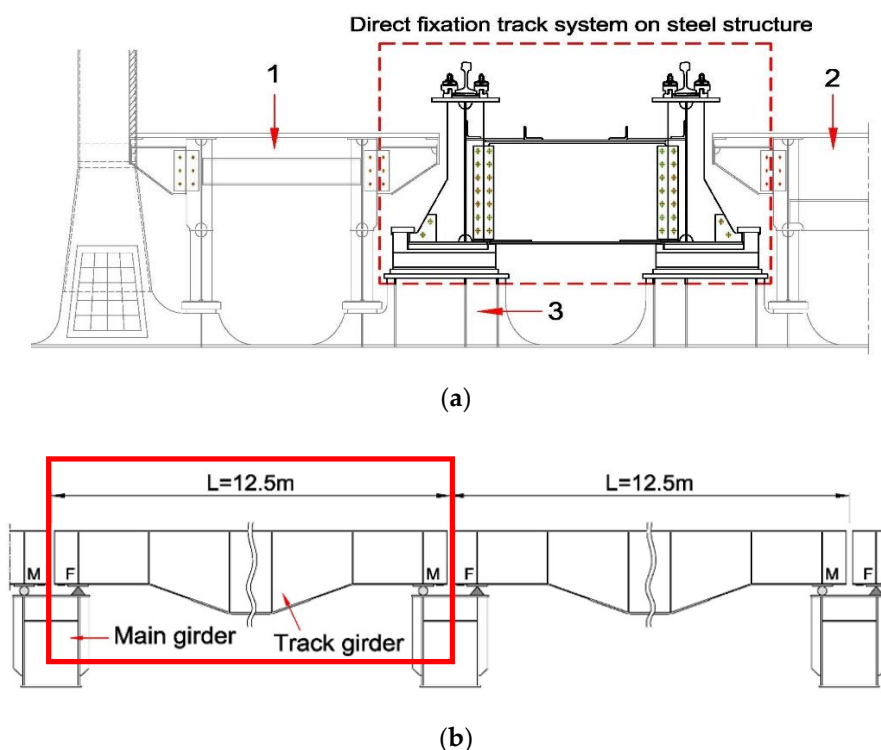


**Figure 3.** Schematics of the direct-fixation track system [12]: (a) cross-sectional view. 1. side bridge inspection passage, 2. center bridge inspection passage, 3. cross beam of the main bridge (truss and cable bridges); (b) side view.

As shown in Figure 3a, the bearing system was discussed with the direct-fixation rail-fastening system in a 12.5 m span installed. The top plate of the line bearing installed in Figure 3b transmits the vertical load and displacement acting on the structure to the low plate and only allows for movement in the bridge axis direction. In addition, the low plate is in direct contact with the top plate and accommodates vertical load and rotation. The structure of the line bearing installed in the Yeongjong Grand Bridge is as shown in Figure 4, and the installation status is as shown in Figure 5.

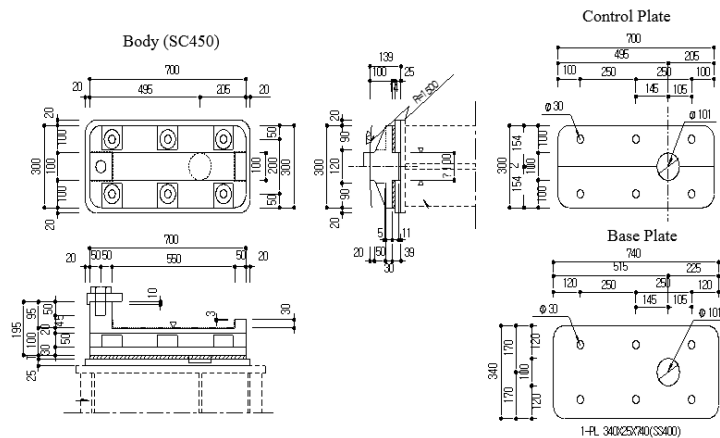


**Figure 4.** Scheme of the line bearing installed in the Yeongjong Grand Bridge.



**Figure 5.** Installation status of the Yeongjong Grand Bridge line bearings.

As shown in Figure 6a, the line bearing easily cracks owing to the impact caused by the movement of vehicles [4,5]. Moreover, the end rotation causes the rail to be deformed, as the rail-fastening system is fixed directly to the bridge deck, and the vertical and compressive forces are generated at the end rail support points to support the rails.



**Figure 6.** Damage of line bearings: (a) the line bearing type for replacement [5]; (b) the corroded top plate of the line bearing [4].

Cylindrical bearings transfer a vertical load and a vertical displacement acting on the structure to lower engineering plastic (EP) cylinders. By installing a device of resistance for a negative reaction force on the side, when the negative reaction occurs, it is transmitted to a side negative-reaction-prevention device to resist the load such as negative reaction and torsion. The vertical load transmitted by the top plate of the cylindrical bearing is passed on to the low plate stably by a central EP cylinder designed to be curved even when rotational displacement occurs. The central EP cylinder is designed in such a manner to minimize the friction coefficient of the contact surface. In addition, the side EP cylinder accommodates the load and displacement acting on the top and bottom locking devices installed on the side of the top plate to minimize the friction coefficient. The load can be transmitted, even if there is a rotational displacement of the top plate. Figure 7 shows the configuration of a plastic engineering cylindrical bearing (ECB), which is one of the cylindrical supports. A comparison of the specifications of the line bearing and the ECB are presented in Table 1.

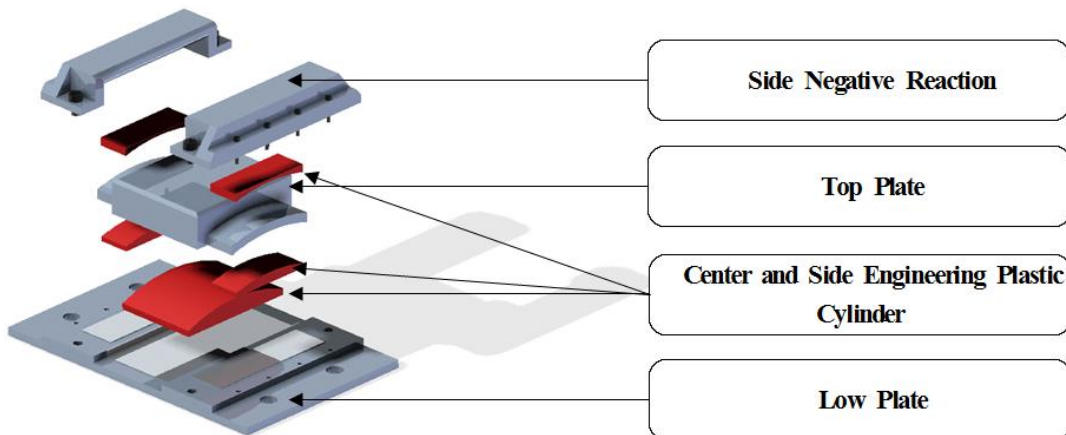


**Figure 7.** Configuration of an engineering cylindrical bearing (ECB).

**Table 1.** Comparison of the specifications of the bearings applicable to the track.

Category	Line Bearing	ECB
Bearing member	Steel	Engineering plastic
Allowable bearing stress	280 MPa	45 MPa
Bearing specification (B × L; B: width, L: length)	60 mm × 60 mm	150 mm × 150 mm
Clearhead under the girder	167 mm	
Bearing capacity	1000 kN	
Beating height	145 mm	145 mm
Rotation angle	0.01 rad	0.06 rad
Negative reaction force key	Absent	Present

According to the bridge design manual (BRDM) (SYSTRA) [14] and railroad design criteria [15], the vertical acceleration of a deck at speeds above 220 km/h should be within 0.35 g, and it must be considered. The Eurocode [16] also states that the vertical acceleration should be within 0.35 g for ballast tracks and within 0.5 g for ballastless tracks. According to UIC 774-3, an end rotation angle caused by a vertical load is an important factor for satisfying the track/bridge interaction behavior; further, it is required to ensure the safety of the ballast by limiting the displacement at the top end of the deck. On the continuous welded rail (CWR), the sum of the distances between the deck top end and banking section and between two successive deck tops is the maximum allowable end-rotation angle [17]. In the evaluation criteria of the dynamic stability of railway bridges in South Korea and Europe, the limitations of end displacements such as the end rotation angle of a concrete slab track bridge are suppressing ballast gravel relaxation and additional increase in rail stress. In a concrete

slab track, the rail stress and the levitation force of the fastening system are specified according to the behavior of the support, because there is no possibility of ballast relaxation. The vertical acceleration limit for the bridge deck is also specified as an item to be evaluated to prevent impact and damage of the support caused by the levitation of the support [15].

### 3. Field Measurements

In this study, displacements were measured at the center and end of the track girders of the Yeongjong Grand Bridge to understand the effect of loads on the track girders. Vertical rail displacements were measured using displacement transducers such as linear variable differential transformers (LVDTs) mounted on a jig anchored on a side bridge inspection passage without influence of train load, as shown in Figure 8. LVDTs (CDP-25 M) has a sensitivity of  $500 \times 10^{-6}/\text{mm}$ , a rated power of  $6.25 \text{ mV/V} \pm 0.3\%$ , and a frequency response of 7 Hz. Displacements were measured and recorded automatically by a computer controlled data acquisition system. In addition, the level of the displacement that occurred at the end of the direct-fixation track of the Yeongjong Grand Bridge was identified and compared with the numerical result. Further, it was used as an input specification for the impact analysis of the track support bearing.

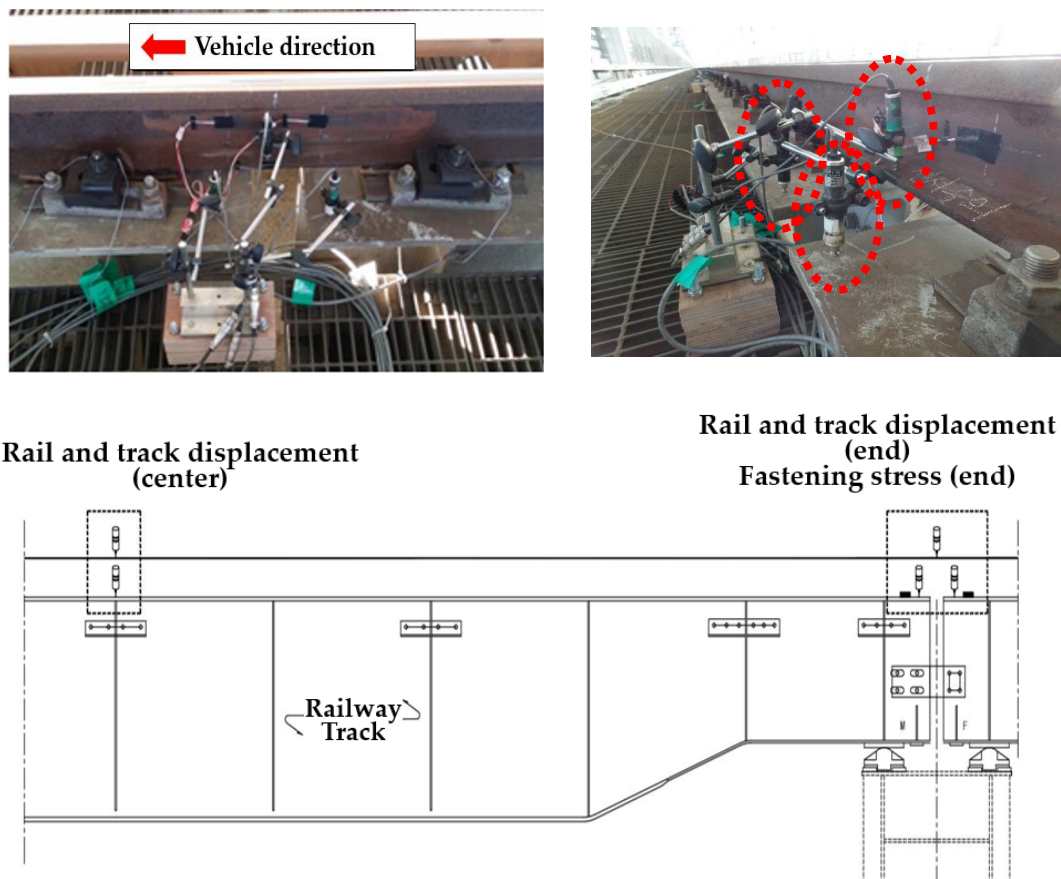


**Figure 8.** View of sensor installation at the track girder center and end.

To examine the upward displacement occurring at the track girder end of the direct-fixation track of the Yeongjong Grand Bridge, the field measurement was carried out by installing a displacement gauge for measuring the displacements of the rail and the track at the center and end of the track girders, as shown in Figure 8. Figure 9 shows an example of the measured waveform.

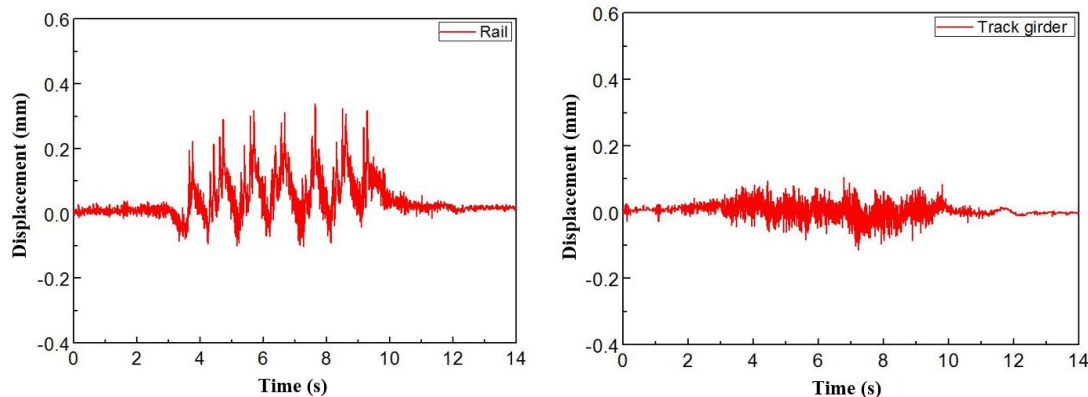


**Figure 9.** Example of a measured waveform Airport Express (AREX) of an end track displacement.

The comparison of the deflection between the rail and the track girder reveals a slight difference in the generated displacement for the 12.5 m girder, as shown in Figure 10. At the end of the direct-fixation track, the rail displacements were 0.24 mm for KTX and 0.15 mm for Airport Express (AREX). At the center of the direct-fixation track, the track girder displacements were 0.31 mm for KTX and 0.18 mm for AREX. The effect of the flexural curvature deformation of the direct-fixation track on the rail and track girder displacements was negligible.

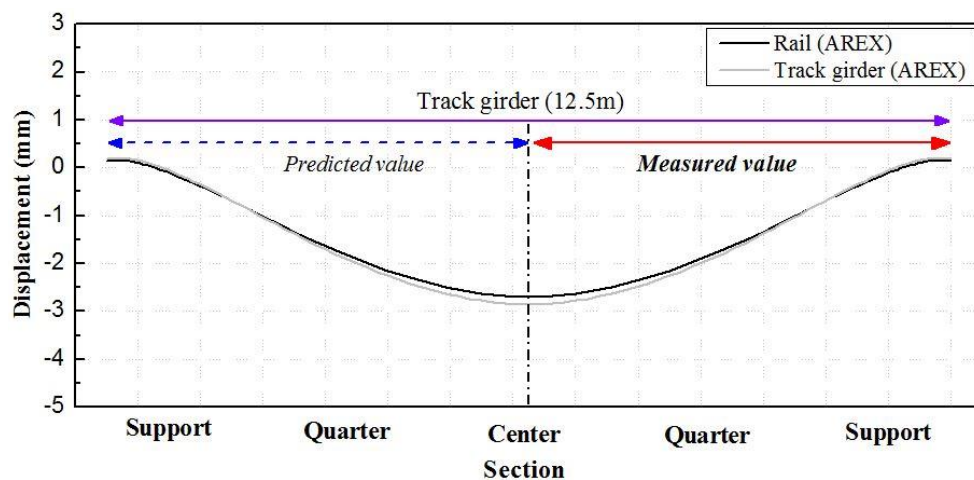


**Figure 10.** Comparison of vertical displacements between the rail and the track.

In this study, field measurements were performed by mounting an accelerometer on top of the rail and track girder to analyze the effect of the vibration occurring in the direct-fixation track of the Yeongjong Grand Bridge on the rail and the track girder. An accelerometer (ARF-50 A) has a frequency response range of DC—130 Hz, a natural frequency of 240 Hz, and a gravimeter with an acceleration of 5.1 g. The accelerometer was used to measure the acceleration of structures subject to vibration. The natural frequency and the damping ratio were estimated using the data measured by the accelerometer.

Figure 11 shows the views of the accelerometer installation for the rail and the track girder. Accelerometers were installed on the rail and the track girder in the same section by the measuring position.

Figure 12 shows an example of the measured waveform of acceleration in the direct-fixation track of the Yeongjong Grand Bridge for track vibration impact evaluation.

The reason for installing one accelerometer was confirmed whether the driving train at accelerations within 0.5 g was accelerated. The vibration level of the current track was analyzed to be up to five times higher than the ballastless track (acceleration less than 0.5 g) using the general elastic rail-fastening

system. It was expected to be susceptible to vibrations and thus damage and impact at the support of the track. In this study, the structural safety and the durability of the line bearing of the track were analyzed using the upward displacement measurement results of the support.



**Figure 11.** Measurement setting for the rail and the track girder: (a) view of accelerometer installation; (b) accelerometer.

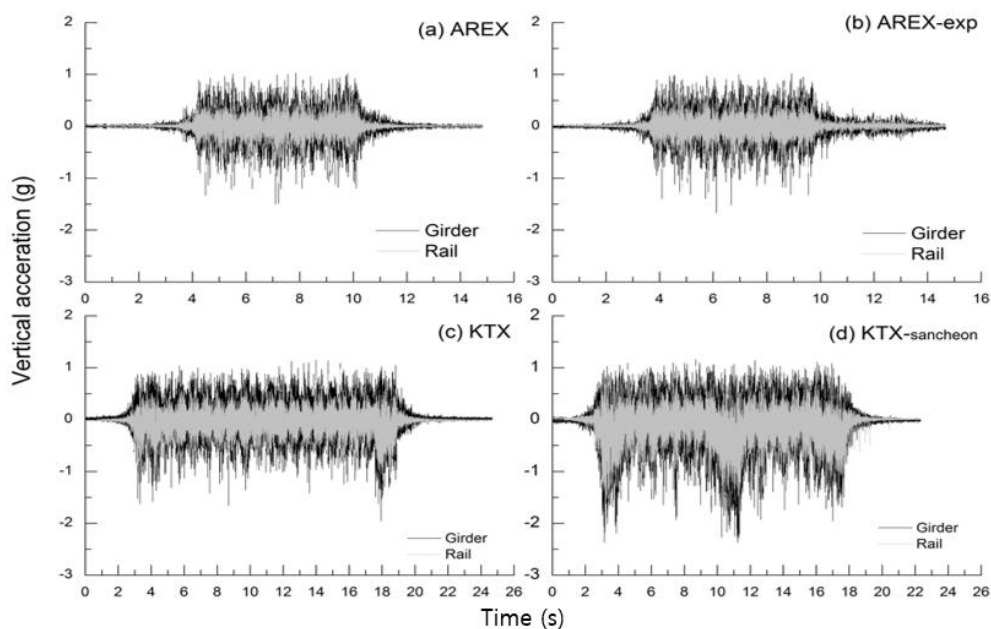


**Figure 12.** Comparison of vertical acceleration between the rail and the track.

#### 4. Finite Element Analysis

##### 4.1. Behavior of the Track Girder Bearing

3D finite element analysis was performed to confirm the structural safety of the vertical and horizontal loads on each form of the bridge bearings. The vertical acceleration acting on the bridge should be within 0.5 g for the bridge decks with concrete tracks, as suggested by the Railway Design Criteria, Eurocode, etc. However, the Yeongjong Grand Bridge has a direct-fixation track and thus, it is not appropriate to apply the allowable vertical acceleration limit for the railway bridge decks with ballast or concrete tracks as presented in the Eurocode or Railway Design Criteria. Therefore, in this study, numerical analysis using field measurement results was performed to verify the adequacy of vibration levels by examining the effect of the vertical acceleration of the direct-fixation track on the structural safety of the supporting point of the track girders. As a result of field measurements,

the current vertical acceleration of the track was about 1 g or more, which exceeded the standard set in the Eurocode and domestic criteria. Therefore, the structural problems of the support bearing due to the higher vertical acceleration of the track were identified, and the effect of the upward displacement of the support on the structural behavior of the line bearing was analyzed.

In the case of the line bearing of track girders on the Yeongjong Grand Bridge, it is simply connected with the upper flange of track girders and there is a distance of 10 mm from the upper girder, as shown in Figure 4.

ANSYS Ver. 17.0 [18] was used as the finite element analysis program, and Solid Edge was used for 3D modeling. Each component of the line bearing model are shown in Figure 13a. Figure 13b shows the ECB component models. Static analysis was performed, and the physical properties are shown in Table 2.

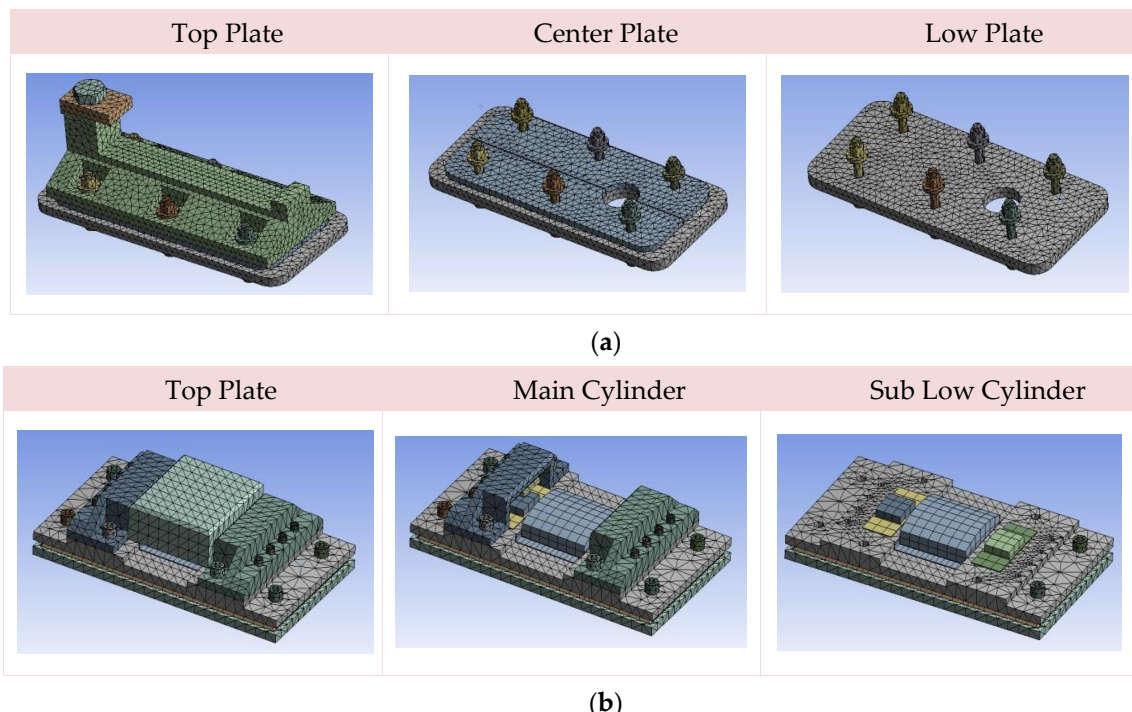


**Figure 13.** Modeling: (a) line bearing; (b) ECB.

**Table 2.** Material Properties of ECB and Line Bearing.

Component	Modulus of Elasticity (MPa)	Poisson's Ratio (MPa)	Tensile Strength (MPa)	Elongation Percentage (%)
ECB	Central and side cylinders (EP)	2000	0.42	70 or more
	Steel (SM355 or SC Mn2A)	200,000	0.30	490 or more
	Bolt (10.9 G)	200,000	0.30	1040 or more
Line bearing	200,000	0.30	450 or more	19 or more

In order to examine the stability of a bearing by applying a vertical load, all contacts for the vertical load were applied as bonded. The contacts of the bearing were applied as frictional by applying a horizontal load.

The lower part of the bearing was fixed under supported conditions, and the maximum vertical and horizontal loads were 700 and 210 kN, respectively. To prevent the rotation of the top plate, the x and y displacements were fixed.

The results of finite element analysis are shown in Figures 14 and 15, and the stresses generated by the members are compared and analyzed in Table 3. In the case of a line bearing, the cross section was small, and the stress of the top plate supported by the line bearing exceeded the yield stress. It was

found that the safety factor for the common load was not satisfactory. Further, the cross-sectional change caused by the plastic deformation occurred in the top support plate upon exceeding the yield stress. The safety factor for the generated stress of the low plate of the line bearing was estimated to be 5.3 times smaller than that of the ECB.

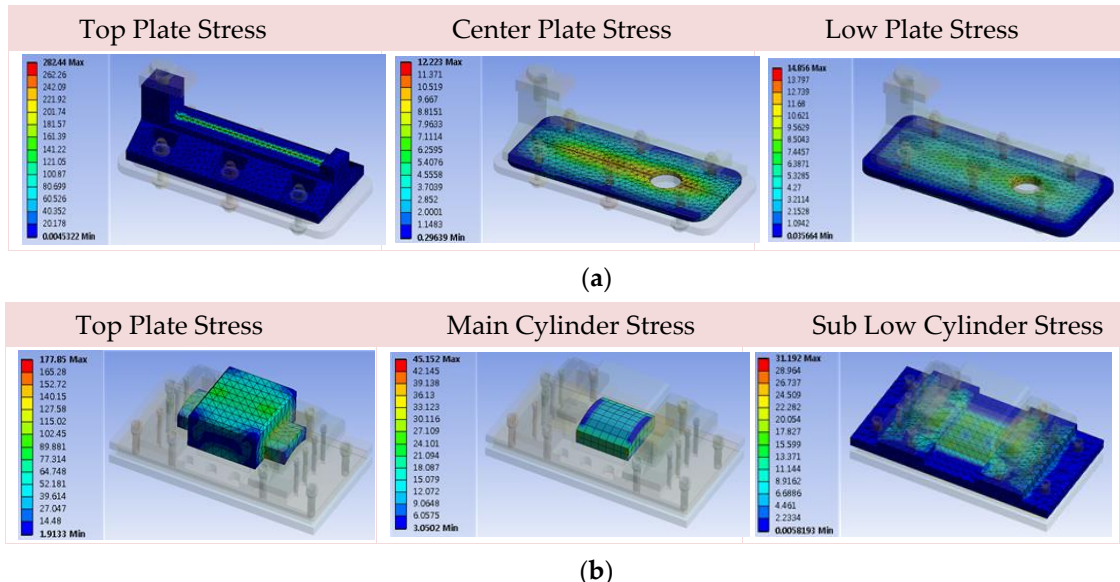


**Figure 14.** Results of finite element analysis (vertical load). (a) Line bearing; (b) ECB.

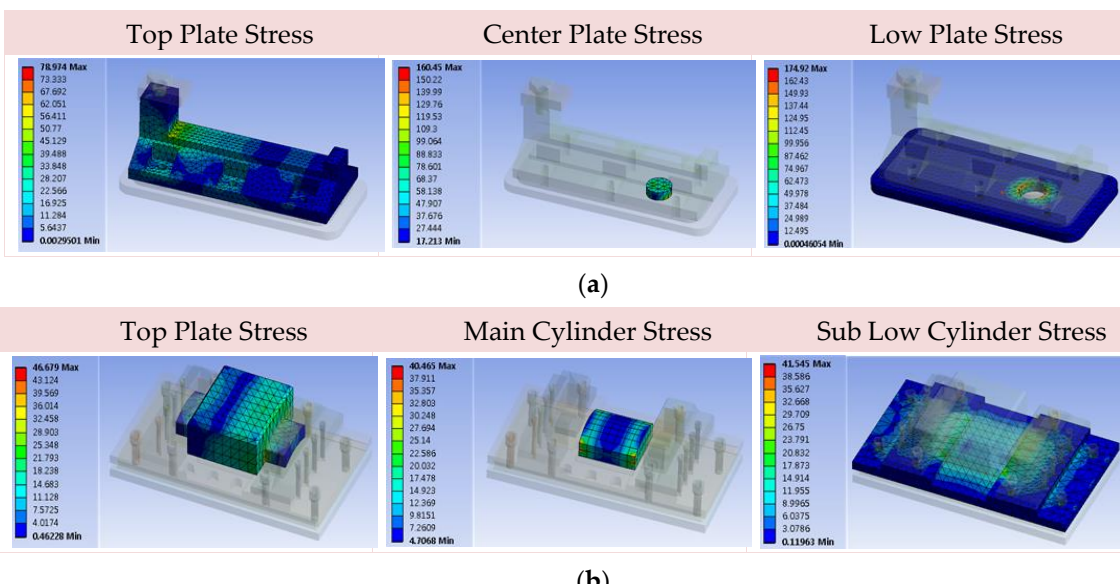


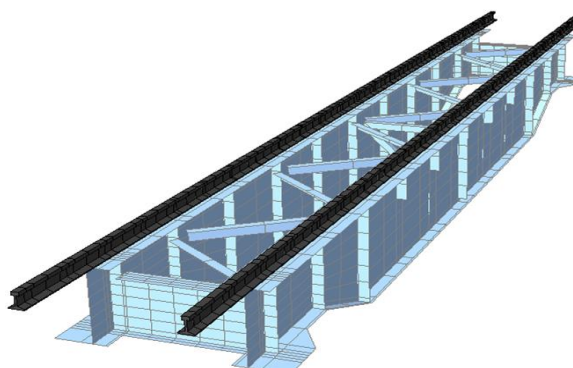
**Figure 15.** Results of finite element analysis (horizontal load): (a) line bearing; (b) ECB.

#### 4.2. Behavior of the Track Girder According to the Bearing Type

To analyze the structural behavior of the track girder according to the bearing type using the numerical model applied to the existing line bearing and ECB, the behavior of the track girder according to the train speed was analytically derived and compared with the field measurement results. To accurately reflect the direct-fixation track girder of the Yeongjong Grand Bridge, the track girder and the vertical stiffener were modeled as 3D shell elements, and the rails, crossbeams, and bracings were modeled as beam elements, as shown in Figure 16. MIDAS Civil [19], a general structural analysis program, was used for finite element analysis.

**Table 3.** Review of stress by member.

Component	Material	Category	Generated Stress (MPa)	Minimum Yield Stress (MPa)	Safety Factor
ECB	Top plate	SM355	Vertical	177.85	295
			Horizontal	46.679	295
	Main cylinder	EP	Vertical	45.152	80
			Horizontal	40.465	80
	Bolt	10.9 G	Vertical	-	-
			Horizontal	24.508	900
Line bearing	Low plate	SM355	Vertical	31.192	295
			Horizontal	41.545	295
	Top plate	SC450	Vertical	282.44	225
			Horizontal	78.974	225
	Control plate	SC450	Vertical	12.233	225
			Horizontal	-	-
	Shear key	SC450	Vertical	-	-
			Horizontal	160.45	225
	Bolt	10.9 G	Vertical	-	-
			Horizontal	57.204	900
	Low plate	SS275	Vertical	14.856	235
			Horizontal	174.92	235
					1.34

**Figure 16.** Numerical modeling of the track.

The boundary conditions were set as listed in Table 4, and the general link was used to apply the direction of bearing behavior, axial rigidity, and damping effects to identify the characteristics of the existing line bearings and ECBs.

**Table 4.** Boundary conditions.

Category	Line Bearing	ECB
Bearing input rigidity	$D_x = 1.0 \times 10^4$ kN/mm; $D_y = 1.0 \times 10^4$ kN/mm	$D_x = 2.4 \times 10^3$ kN/mm; $D_y = 1.0 \times 10^4$ kN/mm
Bearing member configuration	Vertical load support: steel; Horizontal load support: steel	Vertical load support: polyurethane; Horizontal load support: steel
Damping ratio	0.02	0.05

For the load condition, to apply the load of the train acting on the track girder of the Yeongjong Grand Bridge, the time history function was modeled and applied to the time history analysis, considering the effects of the moving loads of Korea Train eXpress, (KTX) train (wheel load and lateral force) and according to the train speed variations, as shown in Figure 17.

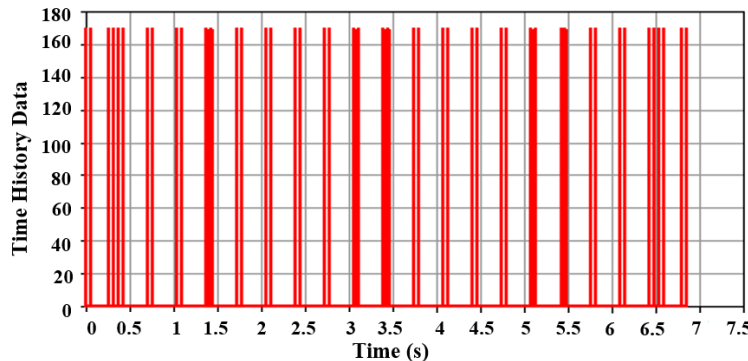


**Figure 17.** KTX time history function example (at a speed of 200 km/h).

To apply the damping value, the damping method was applied as the proportional strain energy. The damping ratio was applied as 1.45% for vertical structures, as 2% for the steel line bearings, and as 5% for the PTFE-based ECBs. In addition, to obtain more accurate results reflecting the effects of the continuous rail and adjacent tracks, it was modeled in three spans, and the results were calculated for the track and the rail located at the center as shown in Figure 18. The results are shown in Table 5.

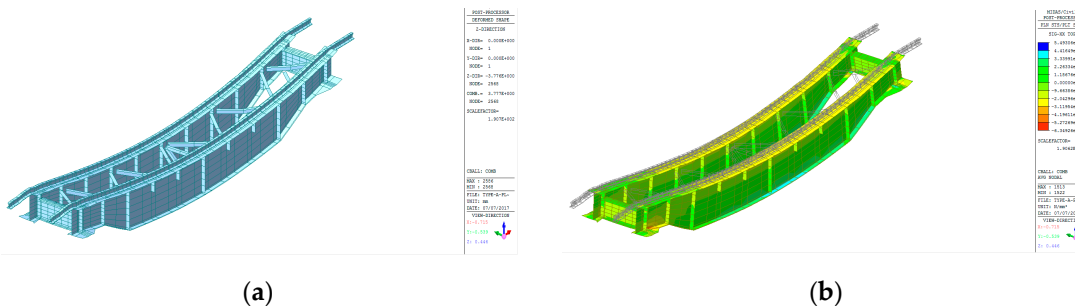


**Figure 18.** Numerical analysis results: (a) maximum vertical displacement: 3.78 mm; (b) maximum track stress: 63.5 MPa.

**Table 5.** Comparison of numerical analysis results.

Category	KTX (90 km/h)		Error (%)	
	Displacement (mm)	Stress (MPa)	Displacement	Stress
Field measurement	3.95	65.0	-	-
Numerical analysis	3.82	63.5	3.29	2.31

As shown in Figure 19a, the vertical displacement of the supporting point of the track girder was not affected by the change of bearings, regardless of the change in speed. ECBs with elastic members for shock absorption were found to have a relatively greater vertical displacement than line bearings. This is due to the elastic displacement (compression displacement) of the elastic material, not the vertical lifting phenomenon of the bearings such as the line bearings. It was confirmed that ECBs can reduce the impact and vibration on the main bridge of the Yeongjong Grand Bridge, supporting the track girder.

As a result of the upward displacement analysis of the track support, the numerical results showed that the upward displacement of the support rarely occurred, regardless of the train speed, as shown in Figure 20. On the other hand, an upward displacement of about 0.21–0.38 mm was measured by field measurements in the track-supporting point with line bearings. The analysis results could underestimate the behavior of the actual track supporting points.

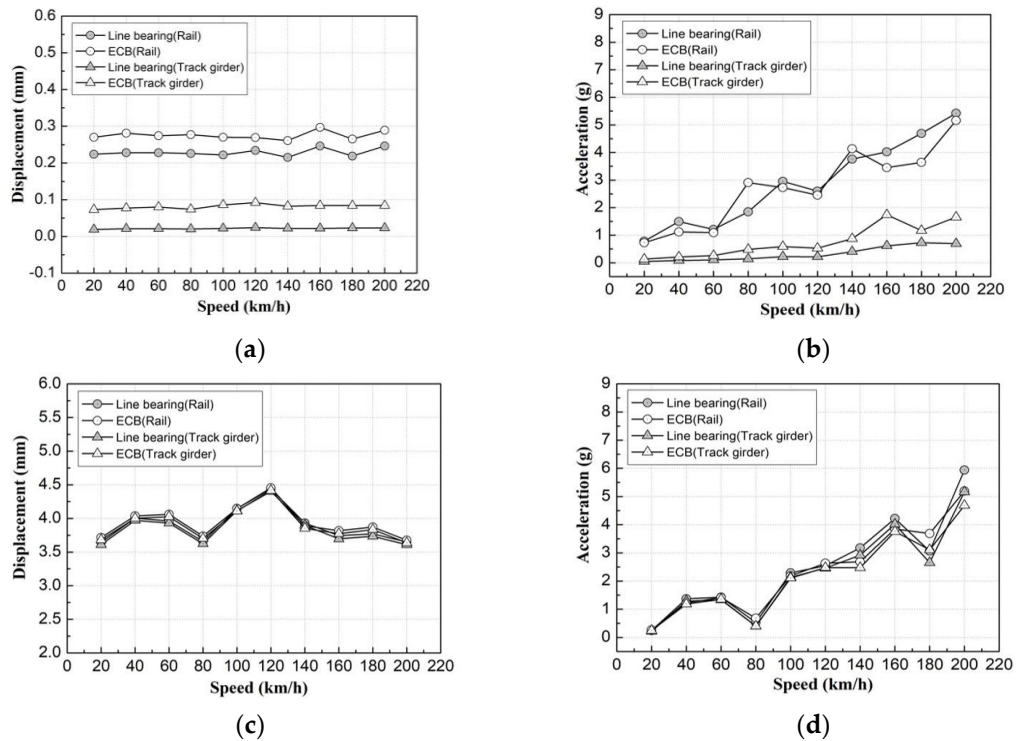


**Figure 19.** Numerical analysis results according to track bearings (vertical direction): **(a)** track support displacement; **(b)** track support acceleration; **(c)** track center displacement; **(d)** track center acceleration.

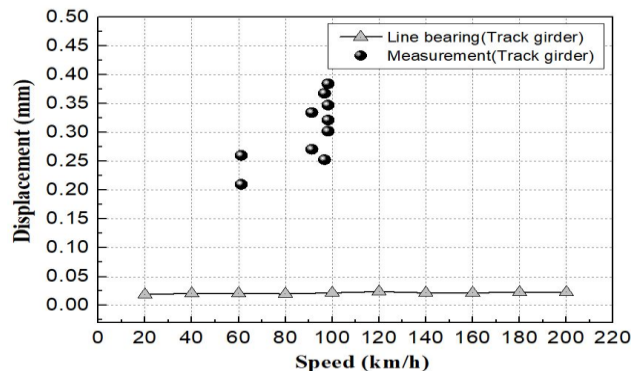


**Figure 20.** Upward displacement of the track support as a function of speed (numerical analysis vs. field measurement result).

#### 4.3. Behavior of the Track Girder Bearing According to Uplift Forces

Finite element analysis was conducted to examine and compare the resistance to negative reaction forces of the existing line bearings and the ECBs. The specifications of the ECBs were designed considering a vertical force of 700 kN, a horizontal force of 210 kN, and a negative reaction force of 140 kN.

ANSYS Ver. 16.2 was used for finite element analysis, and the modeling is shown in Figure 21. The physical properties of the material were shown in Table 2 with the basic assumption that the materials had elastic behavior.

In this analysis, the conditions were defined for the ECB's cylinder contact part of the negative-reaction-force bolt used in each device. For bolts used in line bearings, a frictionless contact condition was defined for the bolt length area entering into the plate hole by a method of externally tightening it with a washer and a nut. The contact condition was considered, since the ECB's cylinder contact part was the portion, where friction occurred when a displacement occurred in the device caused by a horizontal force. However, since this analysis was for the stress distribution due to

the negative reaction force in the vertical direction, a frictionless contact condition was defined for the cylinder contact part. Fastening conditions were defined for all other members.

The finite element analysis results of the bearings are shown in Figure 22 and Table 6.

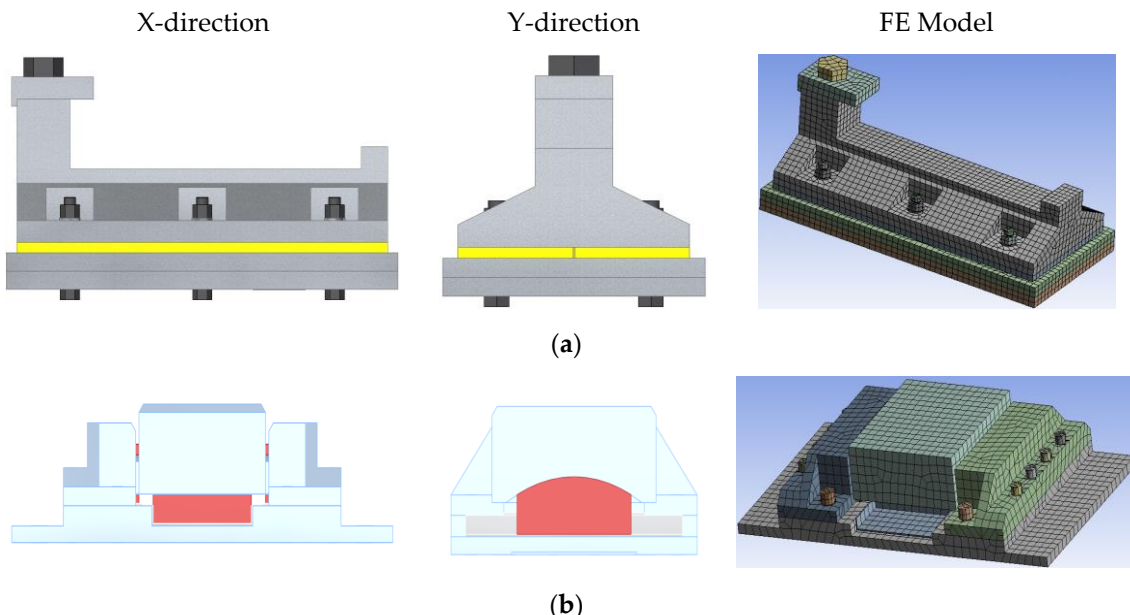


**Figure 21.** Device modeling: (a) line bearing; (b) ECB.

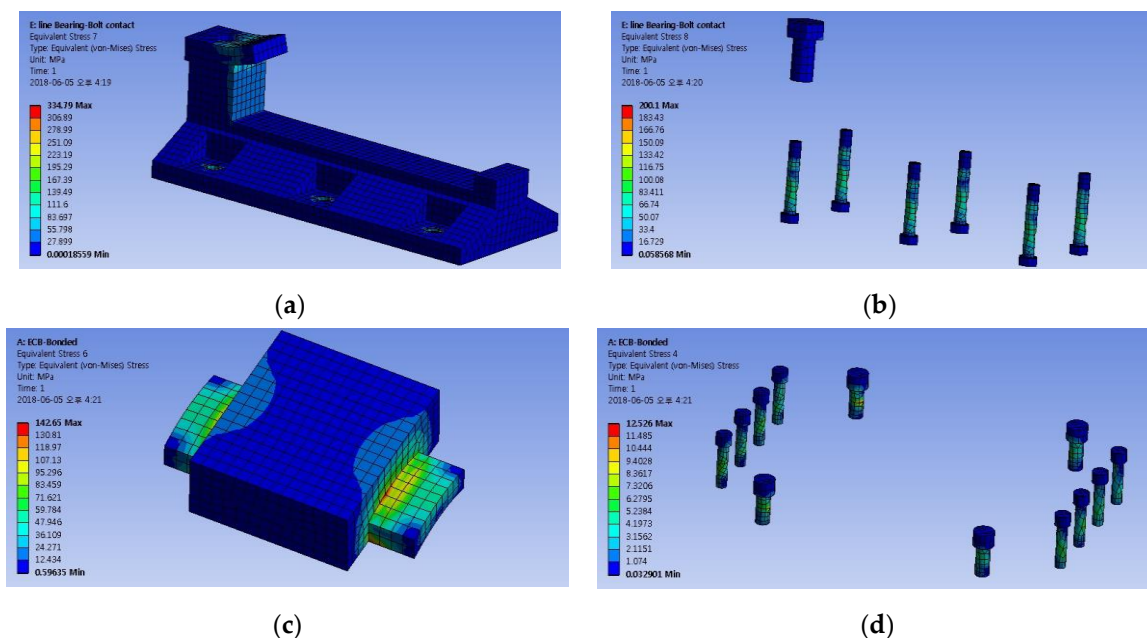


**Figure 22.** Results of the finite element analysis: (a) top plate of the line bearing; (b) bolts of the line bearing; (c) top plate of the ECB; (d) bolts of the ECB.

**Table 6.** Analysis results (at a negative reaction force of 140 kN).

Configuration	Material	Generated Stress (MPa)	Minimum Yield Stress (MPa)	Safety Factor
ECB	Top plate	142.65	295	2.07
	Bolt	10.9 G	900	71.85
Line bearing	Top plate	334.79	225	0.67
	Bolt	200.1	900	4.49

#### 4.4. Impact of the Line Bearing by Uplift

The existing line bearing is connected to the upper girder, and there is a separation from the upper flange of track girder, as shown in Figure 23. Due to the gap of the upper flange of the track girder and the anchoring plate of the line bearing, a negative reaction force could generate the uplift of the track girder ends and the impact of the anchoring plate of the line bearing. The upward displacements on the supporting point of track girder obtained through field measurements, as shown in Figure 20, were set to the loading conditions for the displacement of the shock-induced model analysis. The separation distance experimentally calculated between the anchoring plate of the line bearing and the upper girder was 0.5 mm, as shown in Figure 20.

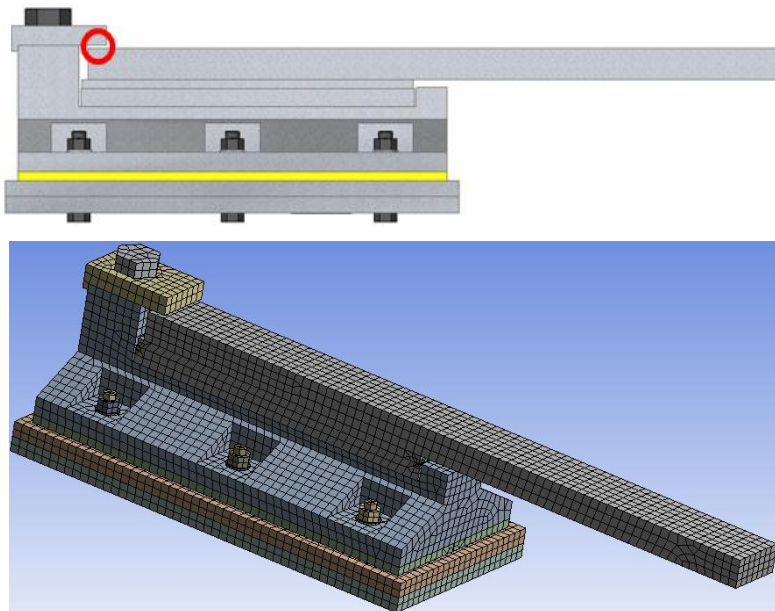


**Figure 23.** Modeled shape and distance from the upper girder.

ANSYS Ver. 16.2 was used for finite element analysis. The analytical modeling is shown in Figure 24. The physical properties of the material were input as shown in Table 2 with the basic assumption that the materials had elastic behavior.

In this analysis, both displacement and rotation were fixed for the boundary condition of the bottom of the device. For the speed load, the speed of the upper flange of the track girder caused by the negative reaction force was assumed to be 0.5 mm/s. In consideration of the separation distance between the anchoring plate of the line bearing and the upper flange of the track girder, a 0.51 mm displacement was set to be caused by the negative reaction force. If the separation distance is set to be the same as the displacement due to the negative reaction force, the impact does not occur, and the stress on the member cannot be confirmed in the analysis program. Therefore, a displacement by the negative reaction force (0.51 mm) greater than the separation distance (0.5 mm) was applied. Since the upper flange of the track girder is a half model, all other displacements and the degree of freedom of rotation except in the vertical direction were fixed for the cut part.

The results of the analysis showed that the displacement and the stress of the upper flange of the track girder and the top plate of the line bearing supporting the upper flange of the track girder were caused by the upward displacement and the downward impact drop phenomenon of the upper flange of the track girder, as shown in Figure 24. The maximum stress (747.31 MPa) generated at the contact of the levitation prevention key and the upper flange of the track girder significantly exceeded the yield stress of the steel (225 MPa). It was analyzed that the upward displacement of the track with the line bearing could result in the damage of the line bearing structure and the deterioration of durability.

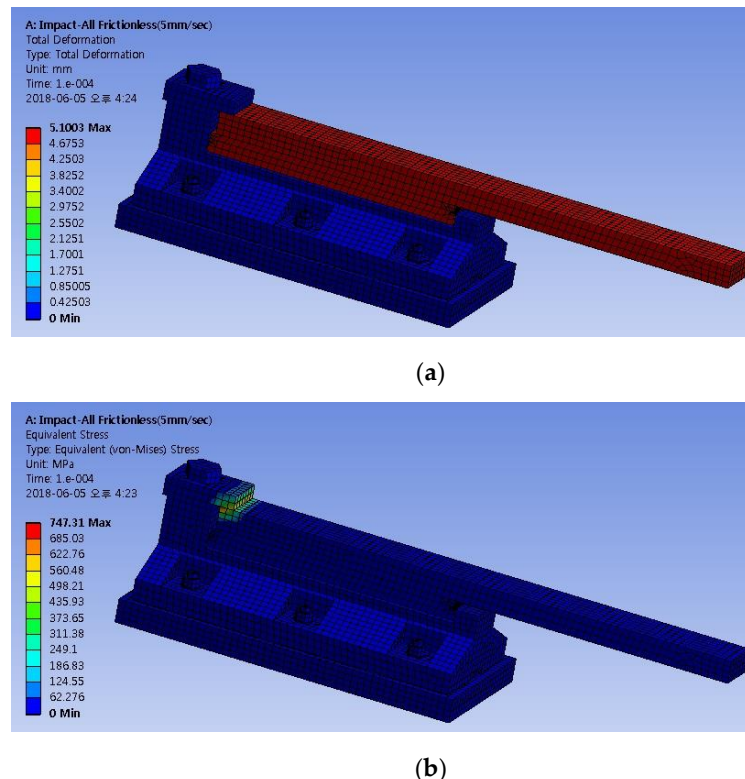


**Figure 24.** Results of finite element analysis for line bearing: (a) girder displacement; (b) stresses in the anchoring plate of the line bearing and the girder by impact.

## 5. Conclusions

This study aimed to solve the problems of the line bearings used in the Yeongjong Grand Bridge in the railway section. Field measurements and numerical analysis were performed to predict the behavior of track and bridge structures, when the line bearings were replaced with cylindrical bearings. In addition, the dynamic behavior of the track–bridge system during the train service was analyzed, and the results are as follows.

The line bearings are steel bearings, which are not supposed to have great vertical displacement owing to the driving of vehicles. However, as a result of the field measurement suggested in the previous studies, it was found that significant displacement occurred in the vertical direction.

As the result of the finite element analysis, for a line bearing, the cross section was small, and the stress of the upper plate supported by the line bearing exceeded the yield stress of the material. The change in the position of the track support due to the change in the cross section of the top plate caused the change in the height of the track rail surface. Further, the safety factor against the generated stress of the line bearing under the horizontal load was estimated to be 5.3 times smaller than that of the ECB. The 3D modeling of the Yeongjong Grand Bridge compared with the field measurement results, showed an error of 3.29% for the displacement and an error of 2.31% for the stress. It turned out to be possible to predict the behavior of railway tracks through finite element analysis.

After applying ECBs instead of the existing line bearings, the displacement was decreased by 93%, and the acceleration was decreased by 82%, indicated in the results of the finite element analysis. In addition, the central displacement was decreased by 45%, and the acceleration was decreased by 82%. Therefore, the existing line bearings were found to have dynamic instability in terms of lateral behavior, as the train speeded up. It was confirmed that the structural stability of the track girder with stable lateral behavior could be ensured, and the dynamic stability of the track girder with relatively high vibration could be obtained by applying the ECBs. For line bearings, the levitation prevention key was applied, only when the top plate was lifted by 10 mm or more. The field measurements indicated that about a 0.4 mm displacement

of the track support occurred. The vertical acceleration of the track was also relatively high. Based on the numerical analysis model applied with the upward displacement in the support obtained through the field measurement results, it was demonstrated that the upward displacement occurring in the track could directly affect the structural safety and the durability of the line bearing.

**Author Contributions:** J.-Y.C. contributed to conception and acquisition of data; S.-H.K. wrote the paper and critically revised the paper. All authors have read and agreed to the published version of the manuscript.

**Funding:** This research received no external funding.

**Conflicts of Interest:** The authors declare no conflicts of interest.

## References

1. Choi, D.H.; Choi, J.H.; Lee, J.J. *KCS 24 40 05, Bridge Bearing, Korean Construction Specification*; Korea Construction Standards Center: Gyeonggi-do, Korea, 2016.
2. Kim, D.-K. Maintenance of bridge bearings. *Mag. Korea Ins. Struct. Maint. Insp.* **2001**, *5*, 45–52.
3. Choi, E.S.; Lee, J.S.; Jeon, H.K.; Park, T.; Kim, H.T. Static and dynamic behavior of disk bearings for OSPG railway bridges under railway vehicle loading. *Nonlinear Dyn.* **2010**, *62*, 73–93. [[CrossRef](#)]
4. Chun, G. *Study on Evaluation Criteria for Bridge Bearings (II)*; Technical Report; Korea Infrastructure Safety Corporation: Jinju-si, Korea, 2003.
5. Choi, E.S.; Choi, S.H. Analysis of dynamic behavior of railroad steel bridges according to bridge bearing types. *J. Korean Soc. Railw.* **2012**, *15*, 62–70. [[CrossRef](#)]
6. Yau, J.D.; Wu, Y.S.; Yang, Y.B. Impact response of bridges with elastic bearings to moving loads. *J. Sound Vib.* **2001**, *248*, 9–30. [[CrossRef](#)]
7. Herwig, A.; Brühwiler, E. In-situ dynamic behavior of a railway bridge girder under fatigue causing traffic loading. *Appl. Stat. Probab. Civ. Eng.* **2011**, *1*, 389–396.
8. Pan, Y.; Agrawal, A.K.; Ghosn, M.; Alampalli, S. Seismic fragility of multispan simply supported steel highway bridges in New York State. I: Bridge modeling, parametric analysis, and retrofit design. *J. Bridge Eng. ASCE* **2010**, *15*, 448–461. [[CrossRef](#)]
9. Choi, E.S.; Lee, H.U.; Lee, S.Y. Maintenance and dynamic behavior of advanced spherical bearings under railway open-steel-plate-girder bridges. *J. Korean Soc. Railw.* **2008**, *11*, 165–175.
10. Caprani, C.C.; De Maria, J. Long-span bridges: Analysis of trends using a global database, structure and infrastructure engineering. *Struct. Infrastruct. Eng.* **2020**, *16*, 219–231. [[CrossRef](#)]
11. Chen, Z.; Zhou, X.; Wang, X.; Dong, L.; Qian, Y. Deployment of a smart structural health monitoring system for long-span arch bridges: A review and a case study. *Sensors* **2017**, *17*, 2151. [[CrossRef](#)] [[PubMed](#)]
12. Choi, J.Y.; Chung, J.S.; Kim, J.H.; Lee, K.Y.; Lee, S.G. Evaluation of behavior of direct fixation track and track girder ends on Yeongjong Grand Bridge. *J. Korean Soc. Saf.* **2016**, *31*, 45–51.
13. Choi, J.Y.; Chung, J.S.; Kim, S.H. Experimental study on track-bridge interactions for direct fixation track on long-span railway bridge. *Shock Vib.* **2019**, *2019*, 1903752. [[CrossRef](#)]
14. SYSTRA. *Bridge Design Manual (BRDM) Final Report*; Korea High Speed Rail Construction Authority (KHRC): Daejeon, Korea, 1995.
15. Korea Rail Network Authority. *Railroad Design Criteria (Road Bed)*; Korea Rail Network Authority: Daejeon, Korea, 2013.
16. Telford, T. *EUROCODE 1 Part 2, "Actions on Structures: General Actions-Traffic Loads on Bridges"*; European Committee for Standardization: London, UK, 1992.
17. International Union of Railway. *UIC Code 774-3, Track/Bridge Interaction Recommendations for Calculations*, 2nd ed.; International Union of Railway: Paris, France, 2001.
18. ANSYS Inc. *ANSYS® 2007 ANSYS Workbench 16.2*; ANSYS Inc.: Cannonsberg, PA, USA, 2015.
19. MIDAS Information Technology Co., Ltd. *MIDAS Civil. Analysis Reference*; MIDAS Information Technology Co., Ltd.: Seongnam-si, Korea, 2016.

